Physics Letters B 725 (2013) 115–122

Contents lists available at SciVerse ScienceDirect

Physics Letters B

www.elsevier.com/locate/physletb

Top quark spin correlations and polarization at the LHC: Standard model predictions and effects of anomalous top chromo moments

Werner Bernreuther [a,*], Zong-Guo Si [b]

[a] Institut für Theoretische Physik, RWTH Aachen University, 52056 Aachen, Germany
[b] Department of Physics, Shandong University, Jinan, Shandong 250100, China

ARTICLE INFO

Article history:
Received 10 May 2013
Accepted 24 June 2013
Available online 3 July 2013
Editor: A. Ringwald

Keywords:
Hadron collider physics
Top quark
Spin
New physics
CP violation

ABSTRACT

A number of top-spin observables are computed within the Standard Model (SM), at next-to-leading order in the strong and weak gauge couplings for hadronic top-quark anti-quark ($t\bar{t}$) production and decay at the LHC for center-of-mass energies 7 and 8 TeV. For dileptonic final states we consider the azimuthal angle correlation, the helicity correlation, and the opening angle distribution; for lepton plus jets final states we determine distributions and asymmetries that trace a longitudinal and transverse polarization, respectively, of the t and $\bar{t}$ samples. The QCD-induced transverse polarization of the top quarks leads to an asymmetry of about 8% that should be detectable with existing data. In addition, we investigate the effects of a non-zero chromo-magnetic and chromo-electric dipole moment of the top quark on these and other top-spin observables and associated asymmetries. These observables allow to disentangle the contributions from the real and imaginary parts of these moments.

1. Introduction

Last year the ATLAS Collaboration [1] at the LHC measured the correlation of t and $\bar{t}$ spins in $t\bar{t}$ production at the LHC. The hypothesis of zero spin correlation was excluded at 5.1 standard deviations. (See also the CMS analysis [2].) Previously, the D0 Collaboration [3] found evidence for $t\bar{t}$ spin correlations in events with a significance of more than 3 standard deviations. These experimental results at the LHC and at the Tevatron are in agreement, within uncertainties, with corresponding standard model (SM) predictions, and therefore provide another experimental proof that the top quark behaves like a bare quark that does not hadronize.

In view of these findings, top-spin observables are rather unique tools (as compared to corresponding observables for lighter quarks) for the detailed exploration of, in particular, top-quark pair production (and decay) dynamics, because (future) measurements of angular correlations/distributions induced by $t\bar{t}$ spin correlations or t, $\bar{t}$ polarization can be confronted with reliable perturbative predictions within the SM versus predictions made with new-physics (NP) models.

As to the modelling of new physics effects one may either consider a specific NP model, e.g. the minimal supersymmetric extension of the SM, or use a rather model-independent approach to parameterize possible NP effects in top-quark production and decay. Here we shall use the second approach.

We consider $t\bar{t}$ production at the LHC and subsequent decays into dileptonic and lepton plus jets final states. The aim of this Letter is twofold. On the one-hand we extend our previous SM predictions of a number of $t\bar{t}$ spin-correlation effects at next-to-leading order in the strong and weak gauge couplings [4–6], and of SM-induced longitudinal [7,8] and transverse [9] t and $\bar{t}$ polarization to pp collisions at the LHC at center-of-mass energies of 7 and 8 TeV. In addition, we analyze the effects of a chromo-magnetic and chromo-electric dipole moment of the top quark on $t\bar{t}$ spin correlations and on t and $\bar{t}$ polarization.

Assuming that new physics effects in hadronic $t\bar{t}$ production are induced by new heavy particle exchanges (characterized by a mass scale M) one may construct a local effective Lagrangian $\mathcal{L}_{eff}$ that respects the SM gauge symmetries and describes possible new physics interaction structures for energies $\lesssim M$. Recent analyses include [10–15]. Here we confine ourselves to interactions of mass dimension 5 after spontaneous electroweak symmetry breaking. Then, as is well-known, the new-physics part of $\mathcal{L}_{eff}$ is given in terms of chromo dipole couplings of the top quark to the gluon(s):

$$\mathcal{L}_{eff} = \mathcal{L}_{SM} - \frac{\tilde{\mu}_t}{2}\bar{t}\sigma^{\mu\nu}T^a t G^a_{\mu\nu} - \frac{\tilde{d}_t}{2}\bar{t}i\sigma^{\mu\nu}\gamma_5 T^a t G^a_{\mu\nu}, \tag{1}$$

where $\tilde{\mu}_t$ and $\tilde{d}_t$ are the chromo-magnetic (CMDM) and chromo-electric (CEDM) dipole moment of the top quark, respectively, $G^a_{\mu\nu}$ denotes the gluon field strength tensor, and T^a the generators of

* Corresponding author.
E-mail addresses: breuther@physik.rwth-aachen.de (W. Bernreuther), zgsi@sdu.edu.cn (Z.G. Si).

0370-2693/$ – see front matter
http://dx.doi.org/10.1016/j.physletb.2013.06.051

$SU(3)$ color. In particular, a sizeable non-zero CEDM would signal a new type of CP-violating interaction beyond the Kobayashi–Maskawa CP phase.

It is customary to define dimensionless chromo moments $\hat{\mu}_t$, $\hat{d}_t$ by

$$\tilde{\mu}_t = \frac{g_s}{m_t}\hat{\mu}_t, \qquad \tilde{d}_t = \frac{g_s}{m_t}\hat{d}_t, \tag{2}$$

where m_t denotes the top-quark mass and g_s is the QCD coupling.

There exists an extensive literature on the phenomenology of anomalous top-quark chromo moments in hadronic $t\bar{t}$ production [16–34]. The topic has been revisited recently [35–40] in view of the large samples of $t\bar{t}$ events that have been recorded so far at the LHC. In fact, the analysis of these data samples yields useful direct information[1] on $\hat{\mu}_t$ and $\hat{d}_t$. For instance, a comparison of $\sigma_{t\bar{t}}^{exp}$ with the SM prediction, made in [35], yields a region in the set of couplings $\hat{\mu}_t$, $\hat{d}_t$ that is still allowed. This allowed region is given roughly by $|\hat{\mu}_t| \lesssim 0.03$, $|\hat{d}_t| \lesssim 0.1$. We will use this result in our analysis below, i.e., we use that the moduli of the dimensionless chromo moments of the top quark, if non-zero at all, are markedly smaller than one.

Because the chromo moments $\hat{\mu}_t$ and $\hat{d}_t$ arise from respective form factors in the limit of large M, we slightly extend the framework of (1) in our analysis below and take into account that these form factors may have absorptive, i.e., imaginary parts if the 4-momentum transfer q^2 in a gluon-top vertex is timelike, in particular if $q^2 > 4m_t^2$. Therefore, we use in the following the parameterization

$$\hat{\mu}_t = \mathrm{Re}\,\hat{\mu}_t + i\,\mathrm{Im}\,\hat{\mu}_t, \qquad \hat{d}_t = \mathrm{Re}\,\hat{d}_t + i\,\mathrm{Im}\,\hat{d}_t, \tag{3}$$

and allow for imaginary parts if the 4-momentum transfer $q^2 > 4m_t^2$ in the respective gluon-top vertex. We emphasize that $\hat{\mu}_t, \hat{d}_t$ parameterize by definition only new physics contributions to gtt and $ggtt$ vertices. The dependence on q^2 of $\hat{\mu}_t$, $\hat{d}_t$ depends on the specific new physics model. We assume that $\hat{\mu}_t$, $\hat{d}_t$ are constants. As we consider below only normalized top-spin observables, this assumption does not spoil perturbative unitarity.

In the following section we consider $t\bar{t}$ production and decay into dilepton and lepton plus jets final states at the LHC (7 and 8 TeV). We compute the contributions of $\hat{\mu}_t$, $\hat{d}_t$ to the respective matrix elements that are linear in the chromo moments. This linear approximation is justified by the upper bounds cited above. We show in Section 3 that the contributions of $\mathrm{Re}\,\hat{\mu}_t$, $\mathrm{Re}\,\hat{d}_t$, $\mathrm{Im}\,\hat{\mu}_t$, and $\mathrm{Im}\,\hat{d}_t$ can be disentangled with appropriate $t\bar{t}$ spin correlation and top polarization observables. In addition, we compute also distributions, expectation values, and asymmetries of these spin observables at next-to-leading order in the strong and weak gauge couplings. In particular, we recompute the SM-induced transverse polarization of the t and $\bar{t}$ quarks, an effect that is worth to be measured in its own right.

2. Set-up of the computation

We consider $t\bar{t}$ production at the LHC and subsequent decay into dileptonic final states,

$$pp \to t + \bar{t} + X \to \ell^+\ell'^- + \text{jets} + E_T^{\text{miss}}, \tag{4}$$

and into lepton plus jets final states,

$$pp \to t + \bar{t} + X \to \ell^+ + \text{jets} + E_T^{\text{miss}}, \tag{5}$$

$$pp \to t + \bar{t} + X \to \ell^- + \text{jets} + E_T^{\text{miss}}, \tag{6}$$

where $\ell, \ell' = e, \mu, \tau$. We use the narrow width approximation for the top quark. Within the SM we consider gg, $q\bar{q}$, gq, and $g\bar{q}$ initiated $t\bar{t}$ production at next-to-leading order in the strong and weak couplings, taking the t and $\bar{t}$ spin degrees of freedom fully into account. On-shell top-quark decay is incorporated at next-to-leading order in the strong coupling in a consistent way. Our computational procedure is described in detail in [6]. We refer to this perturbative calculation of the respective parton matrix elements by the acronym NLOW.

As justified above, we take top-quark chromo moments $\hat{\mu}_t, \hat{d}_t$ into account only in the linear approximation in the following. That is, we consider the interference of the leading-order (LO) QCD amplitudes, i.e., the LO amplitudes for gg, $q\bar{q} \to t\bar{t}$ with the corresponding amplitudes that contain a chromo-moment $\hat{\mu}_t$ or $\hat{d}_t$. In the case of $q\bar{q}$ initial states, this interference term $\delta\mathcal{M}_{q\bar{q}}^{NP}$ results from the interference of the SM and the corresponding NP s-channel diagram. As $s > 4m_t^2$, the chromo form factors may have imaginary parts that we take into account. The LO amplitude of $gg \to t\bar{t}$ involves s-, t-, and u-channel diagrams. Only the chromo form factors that are associated with the s-channel diagrams may have an imaginary part. In this way the interference terms $\delta\mathcal{M}_i^{NP}$ $(i = gg, q\bar{q})$ are obtained that depend linearly on $\mathrm{Re}\,\hat{\mu}_t$, $\mathrm{Re}\,\hat{d}_t$, $\mathrm{Im}\,\hat{\mu}_t$, and $\mathrm{Im}\,\hat{d}_t$ and the t, $\bar{t}$ spins. From these terms we extract the NP contributions δR_i^{NP} to the corresponding SM production density matrices computed at NLOW [6]. The production density matrices δR_i^{NP} were computed, quite some time ago, for $\mathrm{Re}\,\hat{d}_t \neq 0$ by [17] and for $\mathrm{Re}\,\hat{\mu}_t$, $\mathrm{Re}\,\hat{d}_t \neq 0$ by [19]. Our analytic results for δR_i^{NP} agree with those of [17,19].

The NP contributions to the parton matrix elements that describe $t\bar{t}$ production and decay into dileptonic and lepton plus jets final states involve also the SM top-quark decay density matrices for $t \to Wb \to \ell\nu b, q\bar{q}'b$ to LO. At this point the following remark is in order. The top-decay vertex $t \to Wb$ may also be affected by new physics interactions that can also be parameterized by anomalous couplings. We use in the following as spin-analyzers of the (anti)top quark only the charged lepton $\ell^\pm$ from $W^\pm$ decay, and we consider below only lepton angular correlations and distributions that are inclusive in the lepton energies. It is known (see e.g. [43–46]) that these observables are not affected by anomalous couplings from top-quark decay if these couplings are small, i.e., if a linear approximation is justified. This is indeed the case in view of the present upper bounds on the moduli of these couplings that can be inferred from the measured W-boson helicity fractions in top-quark decay (cf., e.g., [47]). In other words, the observables that we analyze in the next section are affected only by possible new physics contributions to $t\bar{t}$ production that we parameterize by complex chromo-moments $\hat{\mu}_t$, $\hat{d}_t$.

For the computations below we use the following input parameters: $m_t = 173.1$ GeV, $\Gamma_t = 1.3$ GeV, $m_W = 80.4$ GeV, $\Gamma_W = 2.09$ GeV, $\alpha_s(\mu = m_Z) = 0.112$, and we use the CTEQ6.6M parton distribution functions [48].

The observables of Section 3 involve the following inertial frames: i) The laboratory frame which is defined by using one of the proton beams as the z axis and choosing the orthogonal x and y axes such that a right-handed coordinate system results. ii) The $t\bar{t}$ zero-momentum frame (ZMF) is obtained by a rotation-free boost from the laboratory frame. iii) The t and $\bar{t}$ rest frames are obtained by respective rotation-free boosts from the $t\bar{t}$ ZMF.

[1] For indirect upper bounds on $|\hat{d}_t|$, $|\hat{\mu}_t|$, cf. [41,42].

3. Observables and results

We analyze a set of top-spin observables that allow to disentangle, in the linear approximation for the top chromo moments,[2] the contributions from $\mathrm{Re}\,\hat{\mu}_t$, $\mathrm{Re}\,\hat{d}_t$, $\mathrm{Im}\,\hat{\mu}_t$, and $\mathrm{Im}\,\hat{d}_t$ to the matrix elements of (4)–(6). Because the charged lepton form top decay is the best top-spin analyzer, we consider here only lepton angular correlations and distributions.

For the dileptonic final states (4) we consider the following observables that involve the charged leptons ℓ^+, ℓ'^-: i) The azimuthal angle correlation, the helicity correlation and the opening angle distribution. If the top chromo-moments are non-zero, they receive a contribution proportional to $\mathrm{Re}\,\hat{\mu}_t$. ii) Two CP-odd triple correlations that are sensitive to $\mathrm{Re}\,\hat{d}_t$.

The lepton plus jets final states (5), (6) are the most suitable channels for checking whether or not the t and $\bar{t}$ of the hadronically produced $t\bar{t}$ sample have a sizeable polarization. A non-zero $\mathrm{Im}\,\hat{d}_t$ induces a longitudinal t and $\bar{t}$ polarization which the SM predicts to be very small. A non-zero $\mathrm{Im}\,\hat{\mu}_t$ contributes to the transverse polarization of t and $\bar{t}$ which in the SM is generated predominantly by QCD absorptive parts of the scattering amplitudes.

As it has become customary in experimental analyses to present results also by unfolding data for comparison with predictions made at the level of final state partonic jets and/or leptons, we do not, in the following, apply acceptance cuts to the final states in (4) and (5), (6).

3.1. Observables for tracing $\mathrm{Re}\,\hat{\mu}_t$

We consider the dileptonic final states (4) and analyze first the normalized distribution of the difference of the azimuthal angles of the charged leptons in the laboratory frame [50,51,6], $\Delta\phi = \phi_{\ell^+} - \phi_{\ell^-}$.

$$\sigma^{-1}\frac{d\sigma}{d\Delta\phi} = \sigma^{-1}\frac{d\sigma_{SM}}{d\Delta\phi} + \sigma^{-1}\frac{d\sigma_{NP}}{d\Delta\phi}. \tag{7}$$

As emphasized above, we take into account in $d\sigma_{NP}$ only the contributions linear in the chromo moments. As we compute $d\sigma_{SM}$ to NLO in the SM couplings, we have for the integrated cross section of (4):

$$\sigma = \sigma_{LO} + \sigma_{NLOW} + \sigma_{NP}, \tag{8}$$

where, in the linear approximation, the term σ_{NP} (which is in general not positive) receives only a contribution from $\mathrm{Re}\,\hat{\mu}_t$, i.e., $\sigma_{NP} = \mathcal{O}(\alpha_s^2\,\mathrm{Re}\,\hat{\mu}_t)$.

For the calculation of a ratio like (7) to NLO in the SM couplings one has two options: expanding or not expanding the denominator. We use here as default procedure the first option, which is common practice in higher-order perturbative calculations. We then get for the first term on the right-hand side of (7):

$$\frac{1}{\sigma}\frac{d\sigma_{SM}}{d\Delta\phi} = \frac{1}{\sigma_{LO}}\frac{d\sigma_{LO+NLOW}}{d\Delta\phi} - \frac{\sigma_{NLOW}}{\sigma_{LO}^2}\frac{d\sigma_{LO}}{d\Delta\phi} - \frac{\sigma_{NP}}{\sigma_{LO}^2}\frac{d\sigma_{LO}}{d\Delta\phi} + \mathcal{O}(\alpha_s^2),$$

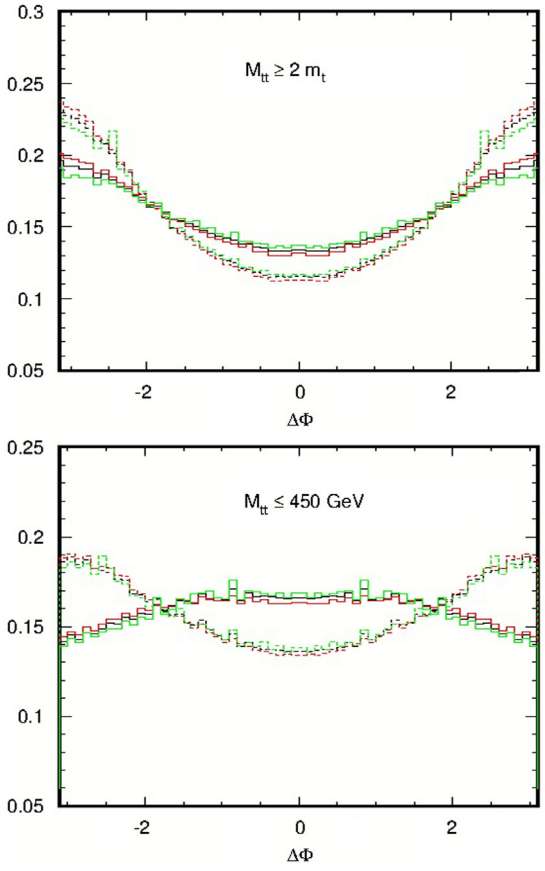

Fig. 1. SM prediction $(\sigma^{-1}d\sigma/d\Delta\phi)_{SM}$ defined in (9), (11) at NLOW for the normalized dilepton $\Delta\phi$ distribution at the LHC (7 TeV). Dashed = uncorrelated, solid = correlated. The chosen scales are $\mu = m_t$ (black), $2m_t$ (red), and $m_t/2$ (green). (Color code in online version only.) Upper plot: distribution without cut on $M_{t\bar{t}}$. Lower plot: distribution for events with $M_{t\bar{t}} \leqslant 450$ GeV.

$$\equiv \left(\frac{1}{\sigma}\frac{d\sigma}{d\Delta\phi}\right)_{SM} - \frac{\sigma_{NP}}{\sigma_{LO}^2}\frac{d\sigma_{LO}}{d\Delta\phi} + \mathcal{O}(\alpha_s^2). \tag{9}$$

Here and below, the label SM refers to the LO and NLOW contributions, i.e., the first two terms in the first line of (9). The contribution in (9) proportional to σ_{NP} will be added to the expanded second term on the right-hand side of (7). The total NP contribution is then given to order $\mathrm{Re}\,\hat{\mu}_t$ by

$$\left(\frac{d\sigma}{\sigma d\Delta\phi}\right)_{NP} \mathrm{Re}\,\hat{\mu}_t \equiv \frac{1}{\sigma_{LO}}\left(\frac{d\sigma_{NP}}{d\Delta\phi} - \frac{\sigma_{NP}}{\sigma_{LO}}\frac{d\sigma_{LO}}{d\Delta\phi}\right). \tag{10}$$

The expanded form (10) is convenient as it is proportional to $\mathrm{Re}\,\hat{\mu}_t$. In summary, we compute the right-hand side of (7) by computing the sum of $(\sigma^{-1}d\sigma/d\Delta\phi)_{SM}$ (cf. (9)) and (10). Notice that the integral $\int d\Delta\phi$ over this sum is one, as it should be.

In Fig. 1 the SM contribution to NLOW of the $\Delta\phi$ distribution is shown[3] for $\sqrt{S_{had}} = 7$ TeV for no cut on the $t\bar{t}$ invariant mass $M_{t\bar{t}}$ and for events with $M_{t\bar{t}} \leqslant 450$ GeV. (This cut was chosen in the experimental analysis [2].) The distributions are symmetric with respect to $\Delta\phi = 0$. For reference, the $\Delta\phi$ distribution is shown in these figures also for the case when the $t\bar{t}$ spin correlations are switched of. These distributions were used in [1,2] for testing the hypothesis "SM, fully correlated" versus "SM, uncorrelated" which led to the exclusion of the second hypothesis with 5.1 s.d. [1]. In

[2] An analysis of the transformation properties of the contributions of $\mathrm{Re}\,\hat{\mu}_t$, $\mathrm{Re}\,\hat{d}_t$, $\mathrm{Im}\,\hat{\mu}_t$, and $\mathrm{Im}\,\hat{d}_t$ to the matrix elements with respect to parity, charge conjugation, and naive time 'reversal' T_N (reversal of spins and 3-momenta) shows that these terms can be disentangled with the top-spin observables used in this section. For a general analysis, see [49].

[3] SM predictions for the distribution of $\Delta\phi$ and of the other observables below for 7 and 8 TeV can be obtained from the authors upon request.

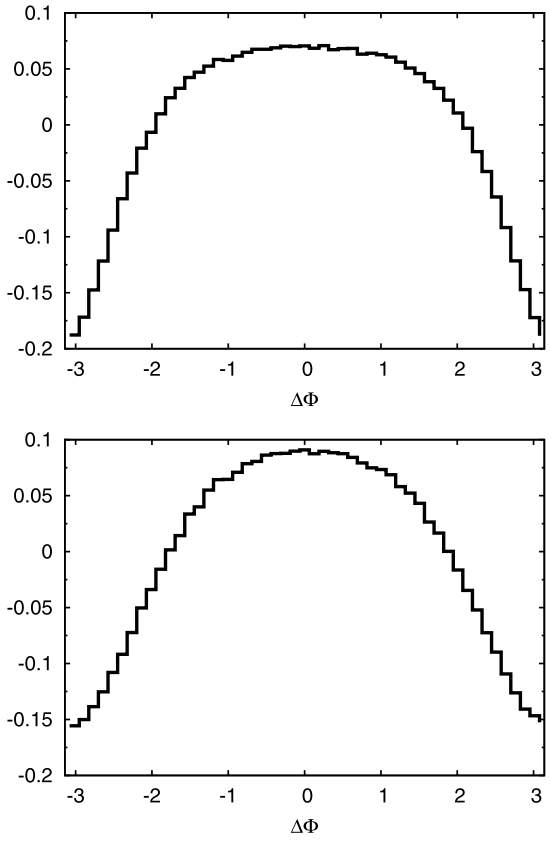

Fig. 2. The contribution $(\sigma^{-1}d\sigma/d\Delta\phi)_{NP}$ defined in (10) to the $\Delta\phi$ distribution at the LHC (7 TeV). Upper plot: no cut on $M_{t\bar{t}}$. Lower plot: events with $M_{t\bar{t}} < 450$ GeV. The thickness of the histogram bars reflects the effects of scale variations $\mu = m_t/2, m_t, 2m_t$.

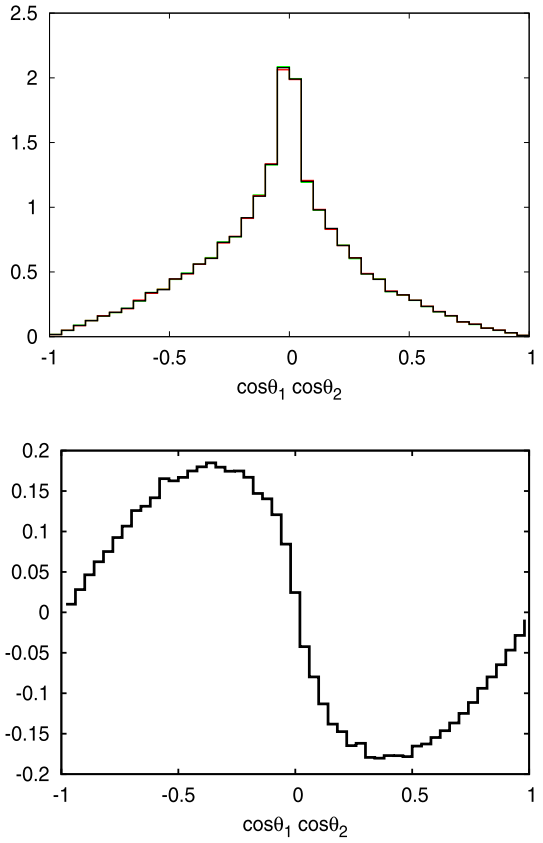

Fig. 3. The normalized distribution of the product $\cos\theta_1 \cos\theta_2$ of the lepton helicity angles, defined in (13) for the LHC (7 TeV). Upper plot: SM prediction at NLOW, $(\sigma^{-1}d\sigma/dO_h)_{SM}$. The chosen scales are $\mu = m_t$ (black), $2m_t$ (red), and $m_t/2$ (green). (Color code in online version only.) Lower plot: NP contribution $(\sigma^{-1}d\sigma/dO_h)_{NP}$. The thickness of the histogram bars reflects the effects of scale variations $\mu = m_t/2, m_t, 2m_t$.

the following, we do no longer consider this option, i.e., we will always consider fully spin-correlated $t\bar{t}$ events, both for SM and NP predictions.

For $\mathrm{Re}\,\hat{\mu}_t \neq 0$ and $|\mathrm{Re}\,\hat{\mu}_t| \ll 1$ we get

$$\frac{1}{\sigma}\frac{d\sigma}{d\Delta\phi} = \left(\frac{1}{\sigma}\frac{d\sigma}{d\Delta\phi}\right)_{SM} + \left(\frac{1}{\sigma}\frac{d\sigma}{d\Delta\phi}\right)_{NP} \mathrm{Re}\,\hat{\mu}_t. \tag{11}$$

The contribution $(\sigma^{-1}d\sigma/d\Delta\phi)_{NP}$ is shown in Fig. 2 for $\sqrt{S_{had}} = 7$ TeV in the range $-\pi < \Delta\phi \leqslant \pi$ for no cut on $M_{t\bar{t}}$ and for events with $M_{t\bar{t}} \leqslant 450$ GeV. (For $M_{t\bar{t}} > 450$ GeV this contribution has the same shape as those of Fig. 2 and is therefore not shown here.) As expected, these contributions are also symmetric with respect to $\Delta\phi = 0$. (Thus, the SM and NP numbers must be doubled if the range $0 \leqslant \Delta\phi \leqslant \pi$ is considered.) Furthermore, by the above assumption, $|\mathrm{Re}\,\hat{\mu}_t|$ must be sufficiently small such that the sum of the two terms on the right-hand side of (11) is positive. Adding these contributions to the respective correlated SM contributions shown in Fig. 1 we see that a cut on $M_{t\bar{t}}$ is of no advantage. Thus, when the $\Delta\phi$ distribution is used to probe for a non-zero $\mathrm{Re}\,\hat{\mu}_t$ one should use the full sample of dileptonic $t\bar{t}$ events.

One may also probe for a non-zero CMDM $\mathrm{Re}\,\hat{\mu}_t$ with the dileptonic angular correlation in the helicity basis. If no acceptance cuts are applied, one has the well-known a priori form of the double angular distribution

$$\frac{1}{\sigma}\frac{d\sigma}{d\cos\theta_1 d\cos\theta_2} = \frac{1}{4}(1 + B_1\cos\theta_1 + B_2\cos\theta_2 - C\cos\theta_1\cos\theta_2), \tag{12}$$

where, in the helicity basis, $\hat{\ell}_+$ ($\hat{\ell}_-$) is the ℓ^+ (ℓ^-) direction of flight in the t ($\bar{t}$) rest frame, $\hat{\mathbf{k}}_t$ and $\hat{\mathbf{k}}_{\bar{t}} = -\hat{\mathbf{k}}_t$ are the t and $\bar{t}$ directions of flight in the $t\bar{t}$ ZMF, respectively, and $\theta_1 = \angle(\hat{\ell}_+, \hat{\mathbf{k}}_t)$, $\theta_2 = \angle(\hat{\ell}_-, \hat{\mathbf{k}}_{\bar{t}})$. For the experimental analysis it is more convenient to use the one-dimensional distributions [5,6] of the product of the cosines $\mathcal{O}_h \equiv \cos\theta_1\cos\theta_2$, rather than analyzing (12). In the linear approximation for the chromo moments, we get in analogy to (11):

$$\frac{1}{\sigma}\frac{d\sigma}{d\mathcal{O}_h} = \left(\frac{1}{\sigma}\frac{d\sigma}{d\mathcal{O}_h}\right)_{SM} + \left(\frac{1}{\sigma}\frac{d\sigma}{d\mathcal{O}_h}\right)_{NP} \mathrm{Re}\,\hat{\mu}_t. \tag{13}$$

In Fig. 3 the SM contribution to NLOW and the NP contribution to this distribution are shown for $\sqrt{S_{had}} = 7$ TeV, for no cut on $t\bar{t}$. Again, we emphasize that (13) applies to values of $\mathrm{Re}\,\hat{\mu}_t$ such that the distribution is positive. We find that applying an upper or lower cut on $M_{t\bar{t}}$, for instance, $M_{t\bar{t}} \leqslant 450$ GeV or $M_{t\bar{t}} > 450$ GeV, does not increase the sensitivity of this distribution to $\mathrm{Re}\,\hat{\mu}_t$ significantly.

The correlation coefficient C in (13) is given in the helicity basis by

$$C_{hel} = -9\langle\cos\theta_1\cos\theta_2\rangle = C_{hel}^{SM} + C_{hel}^{NP}\,\mathrm{Re}\,\hat{\mu}_t. \tag{14}$$

Our results for C_{hel}^{SM} and C_{hel}^{NP} are given in Table 1. The label 'NLOW, expanded' refers to the computation of C_{hel}^{SM} in analogy to (9). For reference purposes, with regard to experimental analyses, we have determined C_{hel}^{SM} also by not expanding the denominator, i.e., by computing $\langle\mathcal{O}_h\rangle = \int d\sigma_{LO+NLOW}\mathcal{O}_h/(\sigma_{LO} + \sigma_{NLOW})$.

Table 1
The contributions to the spin correlation coefficient C_{hel}, defined in (14), for dileptonic events at the LHC (7 and 8 TeV) and the scale choice $\mu = m_t$. The uncertainties in parentheses result from scale choices $\mu = m_t/2, 2m_t$.

7 TeV	$M_{t\bar{t}} \geqslant 2m_t$	$M_{t\bar{t}} \leqslant 450$ GeV	$M_{t\bar{t}} > 450$ GeV
C_{hel}^{SM} (NLOW) expanded	0.310(6)	0.422(2)	0.203(8)
C_{hel}^{SM} (NLOW) unexpanded	0.295(20)	0.417(10)	0.185(22)
C_{hel}^{NP}	0.980(10)	0.972(14)	0.906(15)
8 TeV			
C_{hel}^{SM} (NLOW) expanded	0.318(5)	0.442(2)	0.205(8)
C_{hel}^{SM} (NLOW) unexpanded	0.304(14)	0.435(5)	0.190(20)
C_{hel}^{NP}	0.964(10)	0.949(13)	0.888(10)

Table 2
The SM and NP contributions to the spin correlation coefficient D, defined in (16) and (17), for dileptonic events at the LHC (7 and 8 TeV) and the scale choice $\mu = m_t$. The uncertainties in parentheses result from scale choices $\mu = m_t/2, 2m_t$.

7 TeV	$M_{t\bar{t}} \geqslant 2m_t$	$M_{t\bar{t}} \leqslant 450$ GeV	$M_{t\bar{t}} > 450$ GeV
D_{SM} (NLOW) expanded	−0.223(4)	−0.332(2)	−0.120(6)
D_{SM} (NLOW) unexpanded	−0.212(12)	−0.323(7)	−0.110(15)
D_{NP}	−1.675(20)	−1.670(17)	−1.613(22)
8 TeV			
D_{SM} (NLOW) expanded	−0.228(5)	−0.336(2)	−0.130(5)
D_{SM} (NLOW) unexpanded	−0.217(11)	−0.330(6)	−0.120(14)
D_{NP}	−1.712(19)	−1.696(14)	−1.653(20)

One may also define an asymmetry which, in the absence of acceptance cuts, is determined by C_{hel}:

$$A_h = \frac{N_{\ell\ell}(\mathcal{O}_h > 0) - N_{\ell\ell}(\mathcal{O}_h < 0)}{N_{\ell\ell}(\mathcal{O}_h > 0) + N_{\ell\ell}(\mathcal{O}_h < 0)} = -\frac{C_{hel}}{4}. \tag{15}$$

Next we consider the opening angle distribution for dileptonic final states [53,54,5,6]:

$$\frac{1}{\sigma}\frac{d\sigma}{d\cos\varphi} = \frac{1}{2}(1 - D\cos\varphi), \tag{16}$$

where $\varphi = \angle(\hat{\ell}_+, \hat{\ell}_-)$ and, as above, $\hat{\ell}_+$ ($\hat{\ell}_-$) is the ℓ^+ (ℓ^-) is direction of flight in t ($\bar{t}$) rest frame. If no acceptance cuts are applied then

$$D = -3\langle\cos\varphi\rangle = D_{SM} + D_{NP}\,\mathrm{Re}\,\hat{\mu}_t \quad \text{for } |\,\mathrm{Re}\,\hat{\mu}_t| \ll 1. \tag{17}$$

An associated asymmetry is

$$A_\varphi = \frac{N_{\ell\ell}(\cos\varphi > 0) - N_{\ell\ell}(\cos\varphi < 0)}{N_{\ell\ell}(\cos\varphi > 0) + N_{\ell\ell}(\cos\varphi < 0)} = -\frac{D}{2}. \tag{18}$$

Our results for the SM (at NLOW) and NP contributions to the correlation coefficient D at the LHC (7 and 8 TeV) are given in Table 2. As in the case of the SM predictions for the helicity correlation C_{hel}^{SM}, we give the predictions for D_{SM} at NLOW both in the expanded and in the unexpanded form.

The distributions (11), (13), and (16) may be used for 1-parameter fits to the respective unfolded experimental distributions that ATLAS or CMS may obtain from the existing 7 and 8 TeV dileptonic data samples. In view of the results given in Tables 1 and 2 one may worry that a significant source of theoretical uncertainty is how the higher-order SM contributions are taken into account. As mentioned above, we advocate to use the expanded form of the normalized distributions for fits to the unfolded data, as this is in the spirit of perturbation theory. With which uncertainty may $\mathrm{Re}\,\hat{\mu}_t$ be measured? The highest sensitivity to this parameter will certainly result from fits to these distributions, which is an experimental task. For instance, CMS has reconstructed ~ 9000 dilepton events ($\ell = e, \mu$) from the 7 TeV (5 fb^{-1}) data [52]. Assuming that the same selection efficiency applies to the 8 TeV data, one expects $\sim 5 \times 10^4$ reconstructed dilepton events from the 8 TeV (20 fb^{-1}) data. These numbers suggest that a statistical error $\delta\,\mathrm{Re}\,\hat{\mu}_t$ below the percent level is feasible; the limiting factor will be the systematic experimental and theoretical uncertainties. A crude estimate may be done with the asymmetries introduced above. They should be rather robust from the experimental point of view, but contain, of course, less information than the underlying distributions. Using for instance the asymmetry (18), which has a rather large lever arm to $\mathrm{Re}\,\hat{\mu}_t$, and assuming that A_φ may be measured at 8 TeV with a combined statistical and systematic uncertainty $\delta A_\varphi = 0.03$, then $\mathrm{Re}\,\hat{\mu}_t$ may be extracted with an uncertainty $\delta\,\mathrm{Re}\,\hat{\mu}_t \simeq 0.04$. Estimates of similar order of magnitude were obtained, using different observables, by [35–38].

3.2. Observables for tracing $\mathrm{Re}\,\hat{d}_t$

A non-zero chromo-electric dipole moment $\mathrm{Re}\,\hat{d}_t$ induces CP-odd transverse $t\bar{t}$ spin correlations [49,54], for instance $(\mathbf{S}_t \times \mathbf{S}_{\bar{t}}) \cdot \hat{\mathbf{k}}_t$ (where $\hat{\mathbf{k}}_t$ is the top-quark direction of flight in the $t\bar{t}$ ZMF). These correlations generate, in the dileptonic decay modes the following CP-odd[4] triple correlations [54]:

$$\mathcal{O}_1 = (\hat{\ell}_+ \times \hat{\ell}_-) \cdot \hat{\mathbf{k}}_t, \qquad \mathcal{O}_2 = \mathrm{sign}\big(\cos\theta_t^*\big)(\hat{\ell}_+ \times \hat{\ell}_-) \cdot \hat{\mathbf{p}}. \tag{19}$$

The unit vectors $\hat{\ell}_+$, $\hat{\ell}_-$ that refer to the charged lepton directions of flight are defined as above (cf. below (12)), while $\hat{\mathbf{p}}$ is the direction of one of the proton beams (i.e., the z axis) in the laboratory frame. The factor $\mathrm{sign}(\cos\theta_t^*)$, where $\cos\theta_t^* = \hat{\mathbf{p}} \cdot \hat{\mathbf{k}}_t$, is the sign of the cosine of the top-quark scattering angle in the $t\bar{t}$ ZMF, is required [49,54] because the gg initial state is Bose symmetric. Without that factor, the second triple correlation in (19) would have essentially no sensitivity to a non-zero $\mathrm{Re}\,\hat{d}_t$.

The range of the correlations (19) is $-1 \leqslant \mathcal{O}_{1,2} \leqslant 1$. Within the SM, the distributions of $\mathcal{O}_{1,2}$ are symmetric around $\mathcal{O}_{1,2} = 0$, i.e., the expectation values $\langle\mathcal{O}_{1,2}\rangle_{SM} = 0$ if no acceptance cuts are applied or if these cuts are CP-symmetric. A non-zero $\mathrm{Re}\,\hat{d}_t$ induces asymmetric distributions.

In the linear approximation, the expectation values of $\mathcal{O}_{1,2}$ are directly proportional to $\mathrm{Re}\,\hat{d}_t$:

$$\langle\mathcal{O}_{1,2}\rangle = c_{1,2}\,\mathrm{Re}\,\hat{d}_t. \tag{20}$$

Putting $\mathrm{Re}\,\hat{d}_t = 1$, these expectation values, i.e. the coefficients $c_{1,2}$ are given, for the LHC at 7 and 8 TeV, in Tables 3 and 4, respectively, without and with a cut on $M_{t\bar{t}}$. In the computation of (20) and (21) we have normalized to σ_{LO}.

Corresponding asymmetries are

$$A_i^{CP} = \frac{N_{\ell\ell}(\mathcal{O}_i > 0) - N_{\ell\ell}(\mathcal{O}_i < 0)}{N_{\ell\ell}} = \frac{9\pi}{16}\langle\mathcal{O}_i\rangle, \quad i = 1, 2. \tag{21}$$

This relation between A_i^{CP} and the corresponding expectation value of $\mathcal{O}_i$ holds if no acceptance cuts are applied, but is valid also if cuts on $M_{t\bar{t}}$ are made [54]. Our predictions for these asymmetries are also collected in Tables 3 and 4.

[4] As $|pp\rangle$ is not a CP eigenstate, a classification with respect to CP is, strictly speaking, not possible. However, as long as the acceptance cuts are CP-symmetric, the SM contributions to the expectation values $\langle\mathcal{O}_i\rangle$ are negligibly small. For a discussion, see [54,6].

Table 3
Several expectation values of observables and asymmetries introduced in the text, without and with a cut on $M_{t\bar{t}}$, for the LHC at 7 TeV. The chosen scale is $\mu = m_t$, the uncertainties in parentheses are due to scale variations between $m_t/2$ and $2m_t$. The numbers are to be multiplied by the respective dimensionless chromo moment.

7 TeV		$M_{t\bar{t}} \geqslant 2m_t$	$M_{t\bar{t}} \leqslant 450$ GeV	$M_{t\bar{t}} > 450$ GeV
$\langle \mathcal{O}_1 \rangle$	$[\mathrm{Re}\,\hat{d}_t]$	−0.397(10)	−0.390(10)	−0.403(10)
A_1^{CP}	$[\mathrm{Re}\,\hat{d}_t]$	−0.702(18)	−0.689(18)	−0.712(18)
$\langle \mathcal{O}_2 \rangle$	$[\mathrm{Re}\,\hat{d}_t]$	−0.172(5)	−0.104(2)	−0.230(4)
A_2^{CP}	$[\mathrm{Re}\,\hat{d}_t]$	−0.304(9)	−0.184(4)	−0.406(7)
$\langle \mathcal{O}_T \rangle_{NP}$	$[\mathrm{Im}\,\hat{\mu}_t]$	−0.044(4)	−0.014(2)	−0.069(5)
A_T^{NP}	$[\mathrm{Im}\,\hat{\mu}_t]$	−0.088(8)	−0.027(4)	−0.137(10)
$\langle \mathcal{O}_T \rangle_{QCD}$		−0.021(1)	−0.042(2)	−0.003(1)
A_T^{QCD}		−0.042(1)	−0.084(4)	−0.006(1)

Table 4
The same as Table 3, for the LHC at 8 TeV.

8 TeV		$M_{t\bar{t}} \geqslant 2m_t$	$M_{t\bar{t}} \leqslant 450$ GeV	$M_{t\bar{t}} > 450$ GeV
$\langle \mathcal{O}_1 \rangle$	$[\mathrm{Re}\,\hat{d}_t]$	−0.415(10)	−0.407(10)	−0.420(10)
A_1^{CP}	$[\mathrm{Re}\,\hat{d}_t]$	−0.734(18)	−0.720(17)	−0.743(17)
$\langle \mathcal{O}_2 \rangle$	$[\mathrm{Re}\,\hat{d}_t]$	−0.180(4)	−0.107(2)	−0.237(4)
A_2^{CP}	$[\mathrm{Re}\,\hat{d}_t]$	−0.318(7)	−0.189(3)	−0.419(7)
$\langle \mathcal{O}_T \rangle_{NP}$	$[\mathrm{Im}\,\hat{\mu}_t]$	−0.038(3)	−0.011(2)	−0.060(5)
A_T^{NP}	$[\mathrm{Im}\,\hat{\mu}_t]$	−0.076(6)	−0.022(3)	−0.120(9)
$\langle \mathcal{O}_T \rangle_{QCD}$		−0.018(3)	−0.038(2)	−0.003(1)
A_T^{QCD}		−0.036(6)	−0.076(3)	−0.005(1)

The highest sensitivity to $\mathrm{Re}\,\hat{d}_t$ would be obtained by fitting the distributions $\sigma^{-1} d\sigma/d\mathcal{O}_i$, which depend linearly on $\mathrm{Re}\,\hat{d}_t$, to the respective unfolded experimental distributions. One may expect to achieve a statistical uncertainty $\delta\,\mathrm{Re}\,\hat{d}_t$ below the percent level (cf. Section 3.1). For a crude estimate we use the above CP asymmetries. If A_1^{CP} can be measured with 3 percent accuracy, then $\mathrm{Re}\,\hat{d}_t$ may be determined with an uncertainty $\delta\,\mathrm{Re}\,\hat{d}_t \simeq 0.04$.

3.3. Longitudinal polarization and $\mathrm{Im}\,\hat{d}_t$

If the chromo-electric dipole moment of the top quark has a non-zero imaginary part, $\mathrm{Im}\,\hat{d}_t \neq 0$, then P- and CP-odd contributions (that are T_N-even) to the $q\bar{q}$- and gg-initiated matrix elements are induced. This leads to a longitudinal polarization of both the t and $\bar{t}$ in the $t\bar{t}$ sample [49,54], for instance with respect to the t and $\bar{t}$ directions of flight in the $t\bar{t}$ ZMF: These CP-odd contributions lead to $\langle \mathbf{S}_t \cdot \hat{\mathbf{k}}_t \rangle = \langle \mathbf{S}_{\bar{t}} \cdot \hat{\mathbf{k}}_{\bar{t}} \rangle \propto \mathrm{Im}\,\hat{d}_t$. The P-violating SM interactions[5] and possibly new P-violating, but CP-conserving interactions also lead to a longitudinal t and $\bar{t}$ polarization – in this case one gets $\langle \mathbf{S}_t \cdot \hat{\mathbf{k}}_t \rangle = -\langle \mathbf{S}_{\bar{t}} \cdot \hat{\mathbf{k}}_{\bar{t}} \rangle$.

A search for a non-zero longitudinal t and $\bar{t}$ polarization is most efficiently made in the lepton + jets decay channels, because i) only one charged lepton is required as analyzer of the t and $\bar{t}$ spin, respectively, and ii) the t and $\bar{t}$ rest frames can be reconstructed quite efficiently for these channels. If one uses the lepton helicity angles introduced below (12), i.e., $\theta_1 = \angle(\hat{\ell}_+, \hat{\mathbf{k}}_t)$ and $\theta_2 = \angle(\hat{\ell}_-, \hat{\mathbf{k}}_{\bar{t}})$, then one obtains, for the reactions (5), (6) the distributions (if no acceptance cuts are applied)

$$\sigma^{-1} \frac{d\sigma}{d\cos\theta_{1,2}} = \frac{1}{2}(1 + B_{1,2}\cos\theta_{1,2}), \tag{22}$$

where

$$B_{1,2} = B_{SM} \pm B_{NP}\,\mathrm{Im}\,\hat{d}_t. \tag{23}$$

[5] As in the case of (19), the contribution of the Kobayashi–Maskawa phase is completely negligible.

Table 5
The SM and NP contributions to the longitudinal t and $\bar{t}$ polarization (23), respectively, for $\mu = m_t$. The uncertainties in parentheses are due to scale variations between $m_t/2$ and $2m_t$.

		$M_{t\bar{t}} \geqslant 2m_t$	$M_{t\bar{t}} \leqslant 450$ GeV	$M_{t\bar{t}} > 450$ GeV
7 TeV:	B_{SM}	0.003(1)	0.001(1)	0.005(1)
	B_{NP}	0.538(4)	0.534(2)	0.542(6)
	$\tilde{B}_{NP}$	0.444(12)	0.521(11)	0.380(12)
8 TeV:	B_{SM}	0.003(1)	0.001(1)	0.005(1)
	B_{NP}	0.531(3)	0.532(2)	0.531(5)
	$\tilde{B}_{NP}$	0.463(10)	0.542(10)	0.402(12)

The longitudinal t and $\bar{t}$ polarization induced by SM parity-violating weak interactions is very small; we collect it for reference in Table 5, where our results for B_{NP} are also listed. (For the computation of B_{SM} we took into account our results [7,8].) In the computation of $B_{1,2}$ we have normalized to σ_{LO}. Acceptance cuts on the transverse momentum and on the rapidity of the charged leptons severely distort the shape of the distributions (22) in the backward region $\cos\theta_{1,2} \leqslant 0$ (cf. e.g. [6]). In order to probe for a non-zero $\mathrm{Im}\,\hat{d}_t$ it may therefore be appropriate in an experimental analysis to measure the distributions (22), both for the ℓ^+ and ℓ^- data samples, only in the forward region and consider the "asymmetry"

$$A_P = \frac{N_{\ell^+}(\cos\theta_1 > 0)}{N_{\ell^+}} - \frac{N_{\ell^-}(\cos\theta_2 > 0)}{N_{\ell^-}} = \frac{1}{2} B_{NP}\,\mathrm{Im}\,\hat{d}_t. \tag{24}$$

Alternatively, one may search for a longitudinal t and $\bar{t}$ polarization with the respect to the direction $\hat{\mathbf{p}}$ of one of the proton beams in the lab frame. In this case $\mathrm{Im}\,\hat{d}_t \neq 0$ leads to

$$\langle \mathrm{sign}(\cos\theta_t^*)\mathbf{S}_t \cdot \hat{\mathbf{p}} \rangle = -\langle \mathrm{sign}(\cos\theta_t^*)\mathbf{S}_{\bar{t}} \cdot \hat{\mathbf{p}} \rangle \propto \mathrm{Im}\,\hat{d}_t, \tag{25}$$

where the factor $\mathrm{sign}(\cos\theta_t^*)$ is required because of the Bose symmetry of the gluon-fusion matrix element squared, cf. Section 3.2. This polarization leads, in the $\ell^\pm$ + jets final states, to non-flat distributions of

$$\cos\tilde{\theta}_1 = \hat{\mathbf{p}} \cdot \hat{\ell}_+, \qquad \cos\tilde{\theta}_2 = -\hat{\mathbf{p}} \cdot \hat{\ell}_-, \tag{26}$$

(notice the minus sign in the definition of $\cos\tilde{\theta}_2$), in analogy to (22). In analogy to (24) one may consider

$$\tilde{A}_P = \frac{N_{\ell^+}(\cos\tilde{\theta}_1 > 0)}{N_{\ell^+}} - \frac{N_{\ell^-}(\cos\tilde{\theta}_2 > 0)}{N_{\ell^-}} = \frac{1}{2} \tilde{B}_{NP}\,\mathrm{Im}\,\hat{d}_t, \tag{27}$$

for $\ell^\pm$ + jets final states, separately for events with $\mathrm{sign}(\cos\theta_t^*) = 1$ and -1. The coefficients $\tilde{B}_{NP}$ are also collected in Table 5.

If no acceptance cuts are made, our results for the distributions (22) and the analogous ones for $\cos\tilde{\theta}_{1,2}$ apply also to dileptonic final states.

The longitudinal top polarization was first measured by the D0 Collaboration [55] at the Tevatron. At the LHC (7 TeV) the longitudinal top polarization p_t was measured in the helicity basis by CMS [52] for dilepton events and by ATLAS [56] for ℓ + jets events. These measurements are compatible with zero and the achieved precision (statistical and systematic uncertainties added in quadrature) is $\delta p_t \simeq 0.05$. Using that the top-spin analyzing power of ℓ^+ is $\kappa_\ell = 1$ to very good approximation [57], the polarization p_t as defined in [52] is related to (22) by $p_t = B_1/2$. From $\delta p_t^{exp} \simeq 0.05$ and (22) one obtains, roughly, the upper bound $|\mathrm{Im}\,\hat{d}_t| \lesssim 0.2$. This bound may be improved by exploration of the 8 TeV data. A sensitivity estimate of similar order of magnitude was obtained by [37].

3.4. Transverse polarization and $\mathrm{Im}\,\hat{\mu}_t$

While the SM-induced longitudinal polarization of the t and $\bar{t}$ quarks of the hadronically produced $t\bar{t}$ sample is very small, their polarization transverse to the scattering plane is of the order of a few percent due to QCD absorptive parts of the $q\bar{q}$- and gg-induced scattering amplitudes. A complete calculation to order α_s^3 of this polarization was made in [9,58]. In addition, this P- and CP-even, T_N-odd polarization receives also a contribution from a non-zero imaginary part of the CMDM of the top quark, $\mathrm{Im}\,\hat{\mu}_t \neq 0$.

Again, the lepton + jets final states are obviously the most suitable ones to measure this effect. Appropriate observables are constructed as follows. We define a vector $\mathbf{n}$ that is perpendicular to the $ij \to t\bar{t}$ scattering plane, $\mathbf{n} = \hat{\mathbf{p}} \times \hat{\mathbf{k}}_t$, and consider, for ℓ^+ (ℓ^-) + jets events, the correlation of the ℓ^+ (ℓ^-) direction of flight in the t ($\bar{t}$) rest frame with $\mathbf{n}$. This is achieved, for the respective final states, with the observables

$$\mathcal{O}_T = \mathrm{sign}\big(\cos\theta_t^*\big)\mathbf{n}\cdot\hat{\ell}_+, \qquad \overline{\mathcal{O}}_T = -\,\mathrm{sign}\big(\cos\theta_t^*\big)\mathbf{n}\cdot\hat{\ell}_-. \tag{28}$$

The factor $\mathrm{sign}(\cos\theta_t^*)$ is necessary for obtaining non-zero expectation values of $\mathcal{O}_T$ and $\overline{\mathcal{O}}_T$, cf. Section 3.2 and[6] [9]. We have

$$\langle\overline{\mathcal{O}}_T\rangle = \langle\mathcal{O}_T\rangle = \langle\mathcal{O}_T\rangle_{QCD} + \langle\mathcal{O}_T\rangle_{NP}, \tag{29}$$

and in the linear approximation for the chromo moments, the NP contribution is directly proportional to $\mathrm{Im}\,\hat{\mu}_t$: $\langle\mathcal{O}_T\rangle_{NP} = c_T\,\mathrm{Im}\,\hat{\mu}_t$. In addition one may consider the asymmetry

$$A_T = \frac{N_\ell(\mathcal{O}_T > 0) - N_\ell(\mathcal{O}_T < 0)}{N_\ell} = 2\langle\mathcal{O}_T\rangle, \tag{30}$$

and likewise for $\overline{\mathcal{O}}_T$, where the equality on the right-hand side holds in the absence of acceptance cuts. Our predictions of the contributions from QCD and from a non-zero $\mathrm{Im}\,\hat{\mu}_t$ to the expectation value (29) and to the asymmetry (30) are collected in Tables 3 and 4, both without and with a cut on the $t\bar{t}$ invariant mass. In the computation of (29) and (30) we have normalized to σ_{LO}.

These results show that for ℓ + jets events with low invariant mass, $M_{t\bar{t}} \leqslant 450$ GeV, the correlations (29) and associated asymmetries are sensitive to the QCD-induced transverse polarization of the t and $\bar{t}$ sample, while events with high-invariant mass, $M_{t\bar{t}} > 450$ GeV, are most suited to search for a non-zero $\mathrm{Im}\,\hat{\mu}_t$.

Plenty of $t\bar{t}$ lepton + jets events were recorded at the LHC. For instance, ATLAS has selected close to 4×10^4 such events ($\ell = e, \mu$) from their 7 TeV data. Thus, one expects $\sim 16 \times 10^4$ such events from the 8 TeV (20 fb^{-1}) data. The ratio of events with $M_{t\bar{t}} \leqslant 450$ GeV and $M_{t\bar{t}} > 450$ GeV is approximately 0.45 : 0.55. Thus, the statistical uncertainty in measuring the asymmetry (30) is expected to be below 1%. If a combined uncertainty $\delta A_T^{exp} \simeq 0.02$ can be achieved, both for low and high $M_{t\bar{t}}$ events, the QCD-induced transverse top polarization can be detected, and $\mathrm{Im}\,\hat{\mu}_t$ may be determined with an uncertainty of $\delta\,\mathrm{Im}\,\hat{\mu}_t \simeq 0.16$. A higher precision can be obtained by exploiting the distributions of (28).

4. Summary

Top-spin observables are becoming a useful tool for the detailed exploration of $t\bar{t}$ production and decay at the LHC. In view of the large $t\bar{t}$ data samples that were recorded by the ATLAS and CMS Collaborations at LHC center-of-mass energies of 7 and 8 TeV and that are presently being analyzed in detail, we have extended our previous NLO SM predictions of a number of top-spin correlation and polarization observables to these energies. In particular we have recomputed the QCD-induced transverse polarization of t and $\bar{t}$ quarks. We have shown that this leads, for ℓ^+ + jets events (and likewise for ℓ^- + jets events) with low $t\bar{t}$ invariant mass to an asymmetry A_T^{QCD} of -8.4% (-7.6%) at 7 TeV (8 TeV). It seems feasible that this effect can be measured – it would be an interesting probe of the $t\bar{t}$ production dynamics.

In addition, we have parameterized possible new physics effects in the hadronic $t\bar{t}$ production matrix elements by complex chromo-magnetic and chromo-electric dipole moments of the top quark. Using the presently available empirical information about these moments, namely, that the moduli of the respective dimensionless moments must be markedly smaller than one, we have analyzed a number of charged lepton angular correlations and distributions that allow to disentangle the effects of a non-zero $\mathrm{Re}\,\hat{\mu}_t$, $\mathrm{Re}\,\hat{d}_t$, $\mathrm{Im}\,\hat{\mu}_t$, and $\mathrm{Im}\,\hat{d}_t$. We expect that the analysis of the available 7 and 8 TeV $t\bar{t}$ data samples by ATLAS and CMS will allow to achieve, at least for the real parts of these dimensionless moments, a sensitivity of a few percent. This would provide significant direct information on whether or not hadronic top-quark production is affected by new interactions at length scales as small as 10^{-18} cm.

[6] Our observables (28) have a significantly higher sensitivity than the corresponding lab-frame observables used in [9].

Acknowledgements

We wish to thank J. Andrea, F. Deliot, F. Höhle, C. Schwanenberger, and E. Yazgan for discussions. The work of W.B. was supported by BMBF and that of Z.G. Si by NSFC and by Natural Science Foundation of Shandong Province.

References

[1] G. Aad, et al., ATLAS Collaboration, Phys. Rev. Lett. 108 (2012) 212001, arXiv:1203.4081 [hep-ex].
[2] CMS Collaboration, report CMS-PAS TOP-12-004.
[3] V.M. Abazov, et al., D0 Collaboration, Phys. Rev. Lett. 108 (2012) 032004, arXiv:1110.4194 [hep-ex].
[4] W. Bernreuther, A. Brandenburg, Z.G. Si, P. Uwer, Phys. Rev. Lett. 87 (2001) 242002, arXiv:hep-ph/0107086.
[5] W. Bernreuther, A. Brandenburg, Z.G. Si, P. Uwer, Nucl. Phys. B 690 (81) (2004) 81, arXiv:hep-ph/0403035.
[6] W. Bernreuther, Z.-G. Si, Nucl. Phys. B 837 (90) (2010) 90, arXiv:1003.3926 [hep-ph].
[7] W. Bernreuther, M. Fuecker, Z.G. Si, Phys. Rev. D 74 (2006) 113005, arXiv:hep-ph/0610334.
[8] W. Bernreuther, M. Fücker, Z.G. Si, Phys. Rev. D 78 (2008) 017503, arXiv:0804.1237 [hep-ph].
[9] W. Bernreuther, A. Brandenburg, P. Uwer, Phys. Lett. B 368 (1996) 153, arXiv:hep-ph/9510300.
[10] J.A. Aguilar-Saavedra, Nucl. Phys. B 812 (2009) 181, arXiv:0811.3842 [hep-ph].
[11] J.A. Aguilar-Saavedra, Nucl. Phys. B 821 (2009) 215, arXiv:0904.2387 [hep-ph].
[12] C. Zhang, S. Willenbrock, Phys. Rev. D 83 (2011) 034006, arXiv:1008.3869 [hep-ph].
[13] J.A. Aguilar-Saavedra, Nucl. Phys. B 843 (2011) 638, arXiv:1008.3562 [hep-ph]; J.A. Aguilar-Saavedra, Nucl. Phys. B 851 (2011) 443 (Erratum).
[14] B. Grzadkowski, M. Iskrzynski, M. Misiak, J. Rosiek, JHEP 1010 (2010) 085, arXiv:1008.4884 [hep-ph].
[15] C. Degrande, J.-M. Gerard, C. Grojean, F. Maltoni, G. Servant, JHEP 1103 (2011) 125, arXiv:1010.6304 [hep-ph].
[16] D. Atwood, A. Aeppli, A. Soni, Phys. Rev. Lett. 69 (1992) 2754.
[17] A. Brandenburg, J.P. Ma, Phys. Lett. B 298 (1993) 211.
[18] D. Atwood, A. Kagan, T.G. Rizzo, Phys. Rev. D 52 (1995) 6264, arXiv:hep-ph/9407408.
[19] P. Haberl, O. Nachtmann, A. Wilch, Phys. Rev. D 53 (1996) 4875, arXiv:hep-ph/9505409.
[20] K.-m. Cheung, Phys. Rev. D 53 (1996) 3604, arXiv:hep-ph/9511260.
[21] K.-m. Cheung, Phys. Rev. D 55 (1997) 4430, arXiv:hep-ph/9610368.
[22] B. Grzadkowski, B. Lampe, K.J. Abraham, Phys. Lett. B 415 (1997) 193, arXiv:hep-ph/9706489.

[23] J.M. Yang, B.-L. Young, Phys. Rev. D 56 (1997) 5907, arXiv:hep-ph/9703463.
[24] K.-i. Hikasa, K. Whisnant, J.M. Yang, B.-L. Young, Phys. Rev. D 58 (1998) 114003, arXiv:hep-ph/9806401.
[25] H.-Y. Zhou, Phys. Rev. D 58 (1998) 114002, arXiv:hep-ph/9805358.
[26] D. Atwood, S. Bar-Shalom, G. Eilam, A. Soni, Phys. Rept. 347 (2001) 1, arXiv:hep-ph/0006032.
[27] B. Lillie, J. Shu, T.M.P. Tait, JHEP 0804 (2008) 087, arXiv:0712.3057 [hep-ph].
[28] S.K. Gupta, G. Valencia, Phys. Rev. D 81 (2010) 034013, arXiv:0912.0707 [hep-ph].
[29] S.K. Gupta, A.S. Mete, G. Valencia, Phys. Rev. D 80 (2009) 034013, arXiv:0905.1074 [hep-ph].
[30] Z. Hioki, K. Ohkuma, Eur. Phys. J. C 65 (2010) 127, arXiv:0910.3049 [hep-ph].
[31] Z. Hioki, K. Ohkuma, Phys. Rev. D 83 (2011) 114045, arXiv:1104.1221 [hep-ph].
[32] D. Choudhury, P. Saha, Pramana 77 (2011) 1079, arXiv:0911.5016 [hep-ph].
[33] F. Bach, T. Ohl, Phys. Rev. D 86 (2012) 114026, arXiv:1209.4564 [hep-ph].
[34] E. Gabrielli, A. Racioppi, M. Raidal, H. Veermae, Phys. Rev. D 87 (2013) 054001, arXiv:1212.3272 [hep-ph].
[35] Z. Hioki, K. Ohkuma, Phys. Lett. B 716 (2012) 310, arXiv:1206.2413 [hep-ph].
[36] C. Englert, A. Freitas, M. Spira, P.M. Zerwas, Phys. Lett. B 721 (2013) 261, arXiv:1210.2570 [hep-ph].
[37] S.S. Biswal, S.D. Rindani, P. Sharma, arXiv:1211.4075 [hep-ph].
[38] M. Baumgart, B. Tweedie, JHEP 1303 (2013) 117, arXiv:1212.4888 [hep-ph].
[39] H. Hesari, M.M. Najafabadi, arXiv:1207.0339 [hep-ph].
[40] M. Baumgart, B. Tweedie, arXiv:1303.1200 [hep-ph].
[41] R. Martinez, J.A. Rodriguez, Phys. Rev. D 55 (1997) 3212, arXiv:hep-ph/9612438.
[42] J.F. Kamenik, M. Papucci, A. Weiler, Phys. Rev. D 85 (2012) 071501, arXiv:1107.3143 [hep-ph].
[43] S.D. Rindani, Pramana 54 (2000) 791, arXiv:hep-ph/0002006.
[44] B. Grzadkowski, Z. Hioki, Phys. Lett. B 476 (2000) 87, arXiv:hep-ph/9911505.
[45] B. Grzadkowski, Z. Hioki, Phys. Lett. B 557 (2003) 55, arXiv:hep-ph/0208079.
[46] R.M. Godbole, S.D. Rindani, R.K. Singh, JHEP 0612 (2006) 021, arXiv:hep-ph/0605100.
[47] E. Yazgan, ATLAS Collaboration, CMS Collaboration, arXiv:1304.3324 [hep-ex].
[48] P.M. Nadolsky, H.-L. Lai, Q.-H. Cao, J. Huston, J. Pumplin, D. Stump, W.-K. Tung, C.-P. Yuan, Phys. Rev. D 78 (2008) 013004, arXiv:0802.0007 [hep-ph].
[49] W. Bernreuther, A. Brandenburg, Phys. Rev. D 49 (1994) 4481, arXiv:hep-ph/9312210.
[50] T. Arens, L.M. Sehgal, Phys. Lett. B 302 (1993) 501.
[51] G. Mahlon, S.J. Parke, Phys. Rev. D 81 (2010) 074024, arXiv:1001.3422 [hep-ph].
[52] CMS Collaboration, CMS-PAS-TOP-12-016.
[53] W. Bernreuther, M. Flesch, P. Haberl, Phys. Rev. D 58 (1998) 114031, arXiv:hep-ph/9709284.
[54] W. Bernreuther, A. Brandenburg, M. Flesch, arXiv:hep-ph/9812387.
[55] V.M. Abazov, et al., D0 Collaboration, arXiv:1207.0364 [hep-ex].
[56] ATLAS Collaboration, ATLAS-CONF-2012-133.
[57] A. Brandenburg, Z.G. Si, P. Uwer, Phys. Lett. B 539 (2002) 235, arXiv:hep-ph/0205023.
[58] W.G.D. Dharmaratna, G.R. Goldstein, Phys. Rev. D 53 (1996) 1073.